Electronic Supplementary Material (ESI) for Polymer Chemistry.

Supporting Information

Creation of Micropores by RAFT Copolymerization of Conjugated Multi-Vinyl Cross-Linkers

Chinnadurai Satheeshkumar[1] and Myungeun Seo[1,2,3]*

[1]Graduate School of Nanoscience and Technology, Korea Advanced Institute of Science and Technology (KAIST), Daejeon 34141, Republic of Korea

[2]Department of Chemistry, KAIST, Daejeon 34141, Republic of Korea

[3]KAIST Institute for Nanocentury, KAIST, Daejeon 34141, Republic of Korea

This information includes:

Supporting Scheme S1

Supporting Figures S1 – S20

Supporting Tables S1 – S5

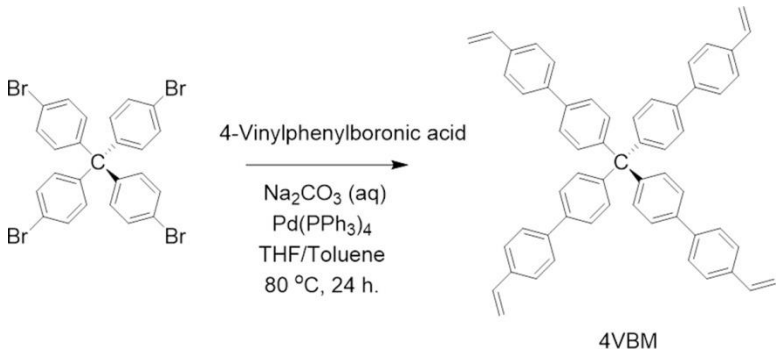

Scheme S1. Synthesis of tetrakis(4-vinylbiphenyl)methane (4VBM)

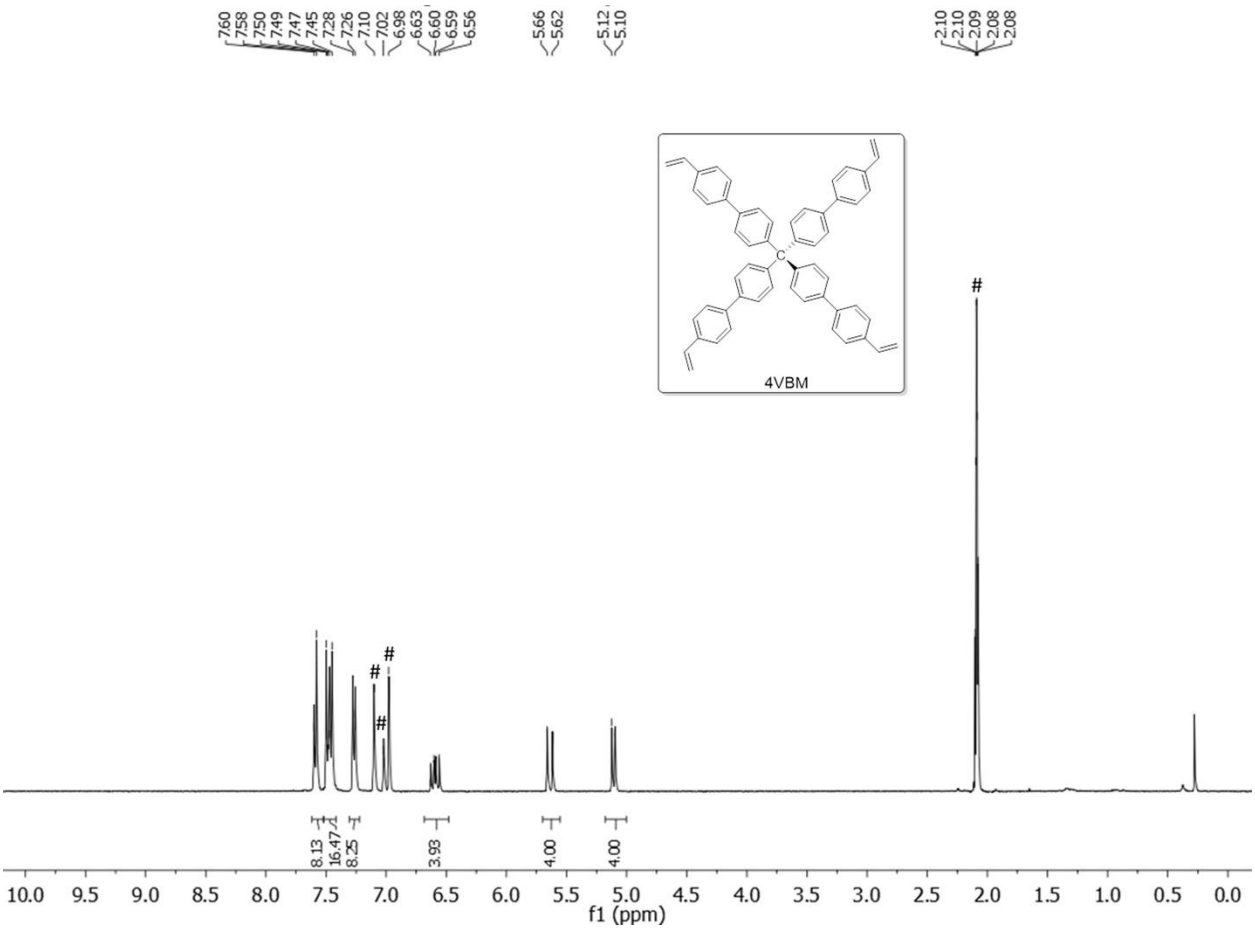

Figure S1. ^{1}H NMR spectrum of 4VBM (400 MHz, toluene-d_8). Peaks corresponding to residual toluene protons are marked with #.

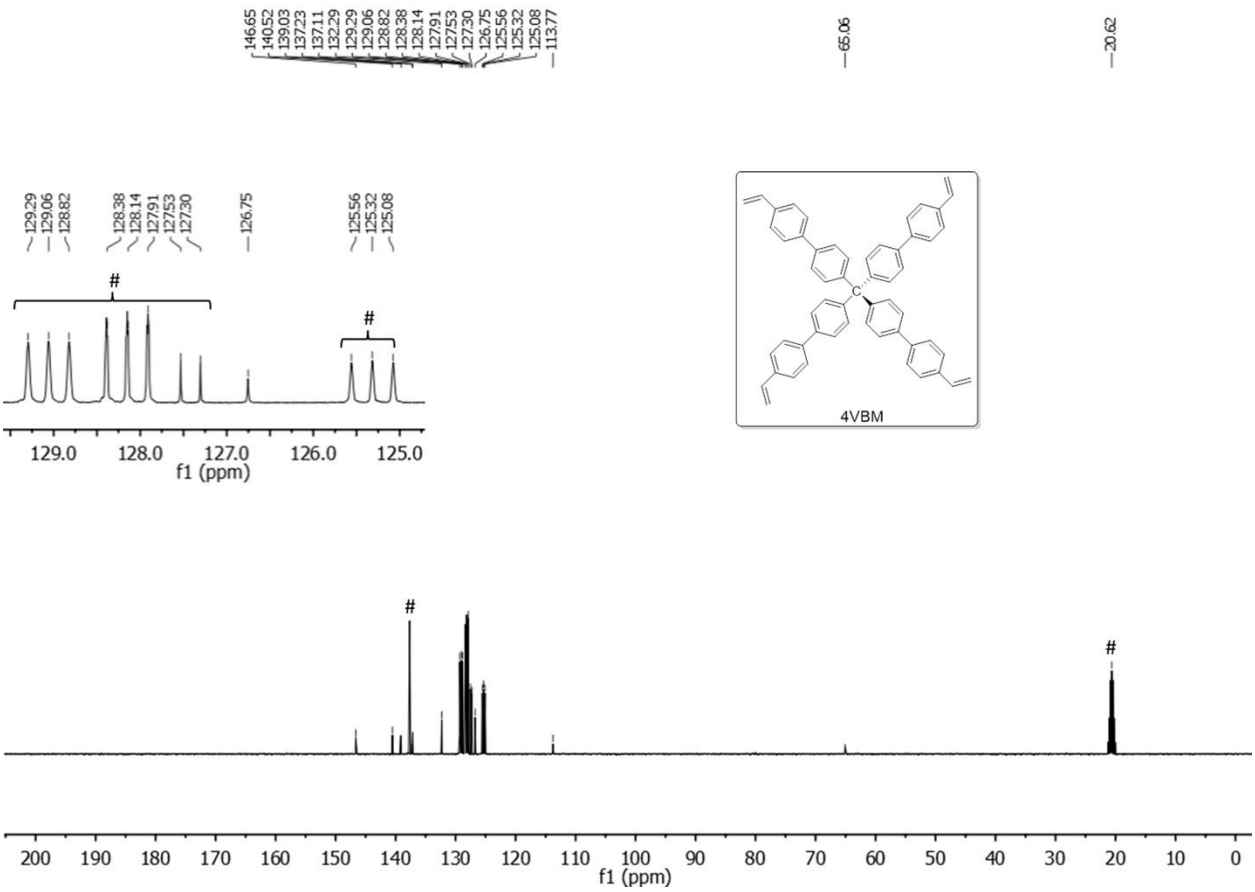

Figure S2. ^{13}C NMR spectrum of 4VBM (100 MHz, toluene-d_8). Peaks corresponding to residual toluene carbons are marked with # (Insert: Expanded ^{13}C NMR spectrum).

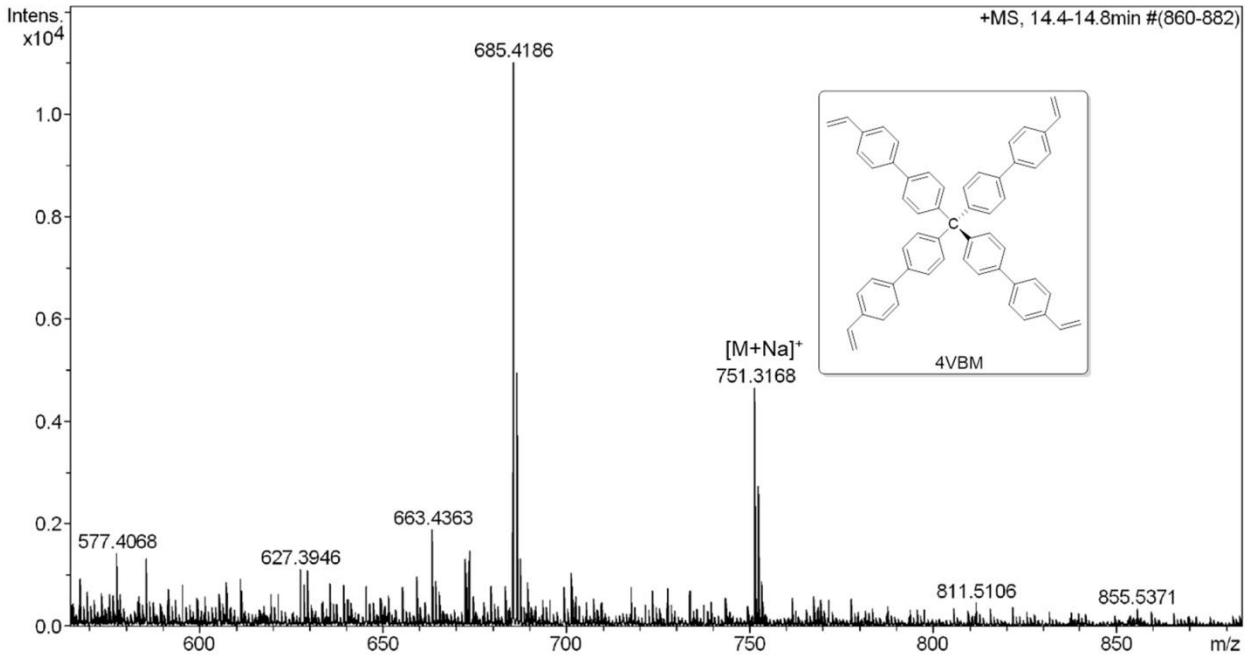

Figure S3. HRMS spectrum of 4VBM.

Table S1. Composition of the polymerization mixtures and yield of PMVCL and P(S-co-MVCL)

Entry	Polymers	Polymerization mixture				Crude yield (%)	Final yield (%)[d]
		Styrene (g)	MVCL (g)	CTA (mg)	DMF (mL)		
1	PDVB[a]	-	0.3	8.4	0.2	62[c]	61
2	P2VBP[a]	-	0.2	3.5	1.2	96	78
3	P3VPB[a]	-	0.15	1.4	0.4	90	69
4	P4VBM[a]	-	0.12	0.6	1.0	81	54
5	P(S-co-DVB)[b]	0.32	0.10	14.1	0.05	72[c]	71
6	P(S-co-2VBP)[b]	0.16	0.08	7.1	0.15	96	92
7	P(S-co-3VPB)[b]	0.11	0.10	5.0	0.25	98	93
8	P(S-co-4VBM)[b]	0.09	0.15	4.0	0.6	97	90

[a][MVCL]:[CTA] = 100:1 (molar ratio)
[b][S]:[MVCL]:[CTA] =80:20:1 (molar ratio)
[c]Insoluble white materials were formed on top of the polymerization mixture and attributed formation of P(S-co-DVB) not mediated by the RAFT CTA.
[d]After DCM washing to remove residual monomers

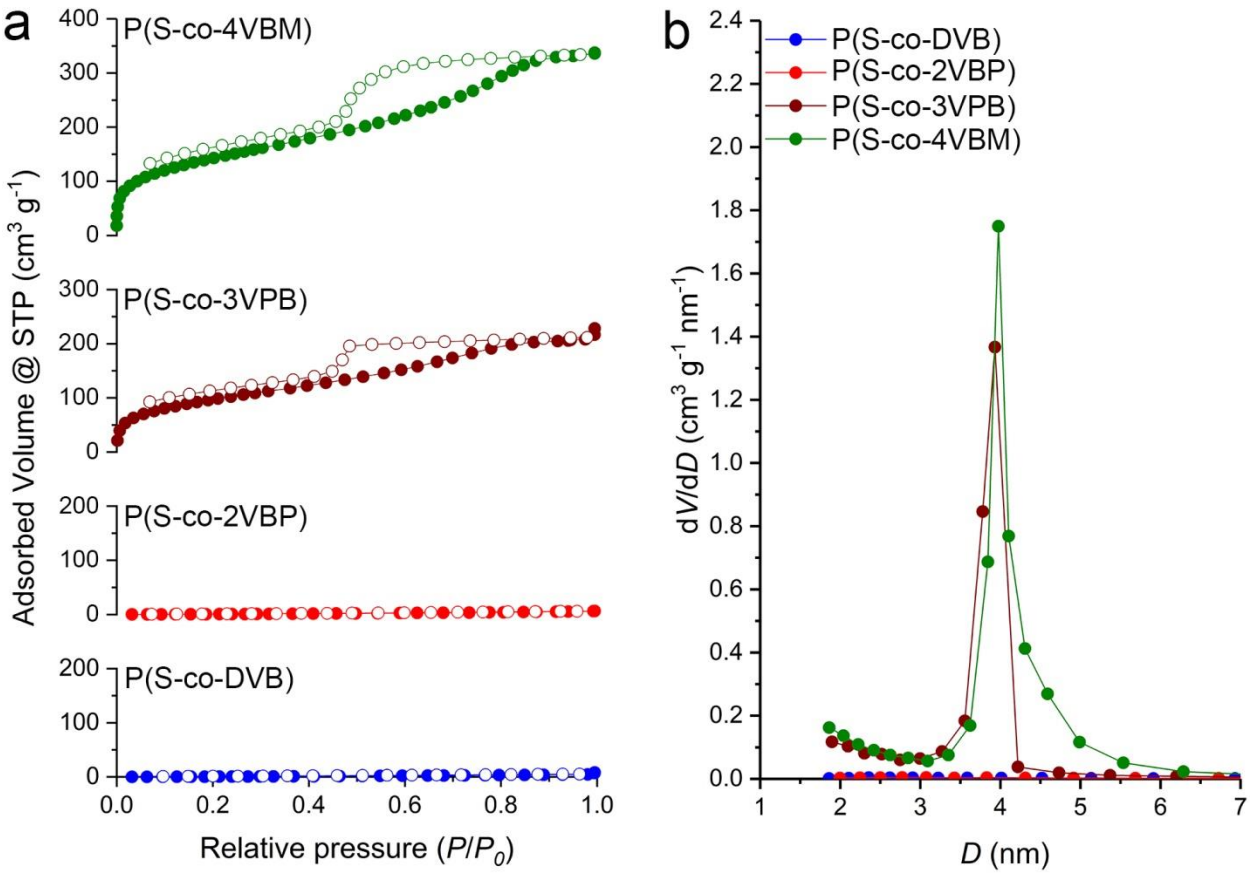

Figure S4. (a) Nitrogen adsorption isotherms of P(S-co-MVCL) synthesized by RAFT copolymerization of styrene with MVCL in the presence DMF as a solvent. Filled circles: adsorption. Empty circles: desorption. (b) BJH pore size distributions of the desorption branch of the isotherms.

Table S2. Pore characteristic of P(S-co-MVCL)

Polymers	Microporosity		Mesoporosity			Whole	
	S_{micro}[a]	V_{micro}[a]	S_{ext}[b]	V_{BJH}[c]	D_{BJH}[c]	S_{BET}[d]	V[e]
P(S-co-DVB)	8	0	8	0.01	3.4	16	0.01
P(S-co-2VBP)	0	0	10	0.01	3.6	8	0.01
P(S-co-3VPB)	57	0.02	291	0.29	3.4	348	0.28
P(S-co-4VBM)	72	0.04	426	0.48	3.5	498	0.44

[a]Micropore surface area and pore volume estimated by t-plot analysis from the points between $0.2 < P/P_0 < 0.45$.
[b]External surface area estimated by t-plot analysis.
[c]Pore volume and mean pore diameter determined by BJH analysis of the desorption branch.
[d]Surface area determined by multipoint BET analysis from the points between $0.05 < P/P_0 < 0.35$.
[e]Pore volume calculated from the point $P/P_0 = 0.95$.

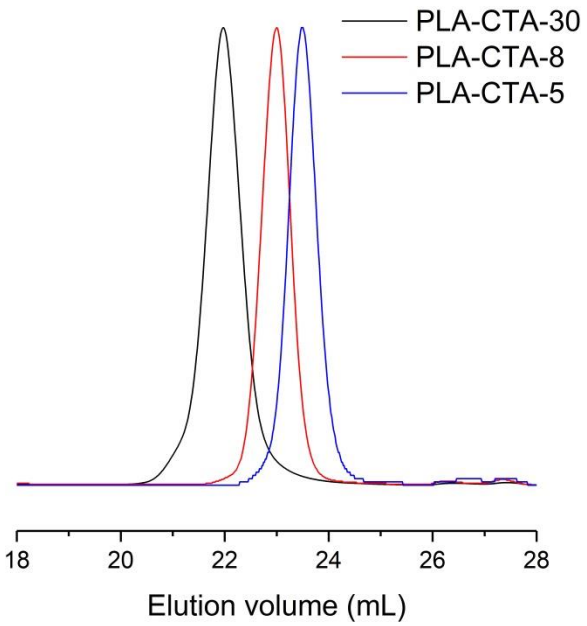

Figure S5. SEC traces of PLA-CTA-30, PLA-CTA-8 and PLA-CTA-5.

Table S3. Characterization of PLA-CTAs

Macro-CTA	$M_{n,NMR}$ (kg mol^{-1})[a]	$M_{n,SEC}$ (kg mol^{-1})[b]	$Đ$[b]
PLA-CTA-30	30	36	1.16
PLA-CTA-8	8	15	1.07
PLA-CTA-5	5	9.7	1.08

[a]Calculated by ^{1}H NMR end group analysis.
[b]Estimated based on linear polystyrene standards.

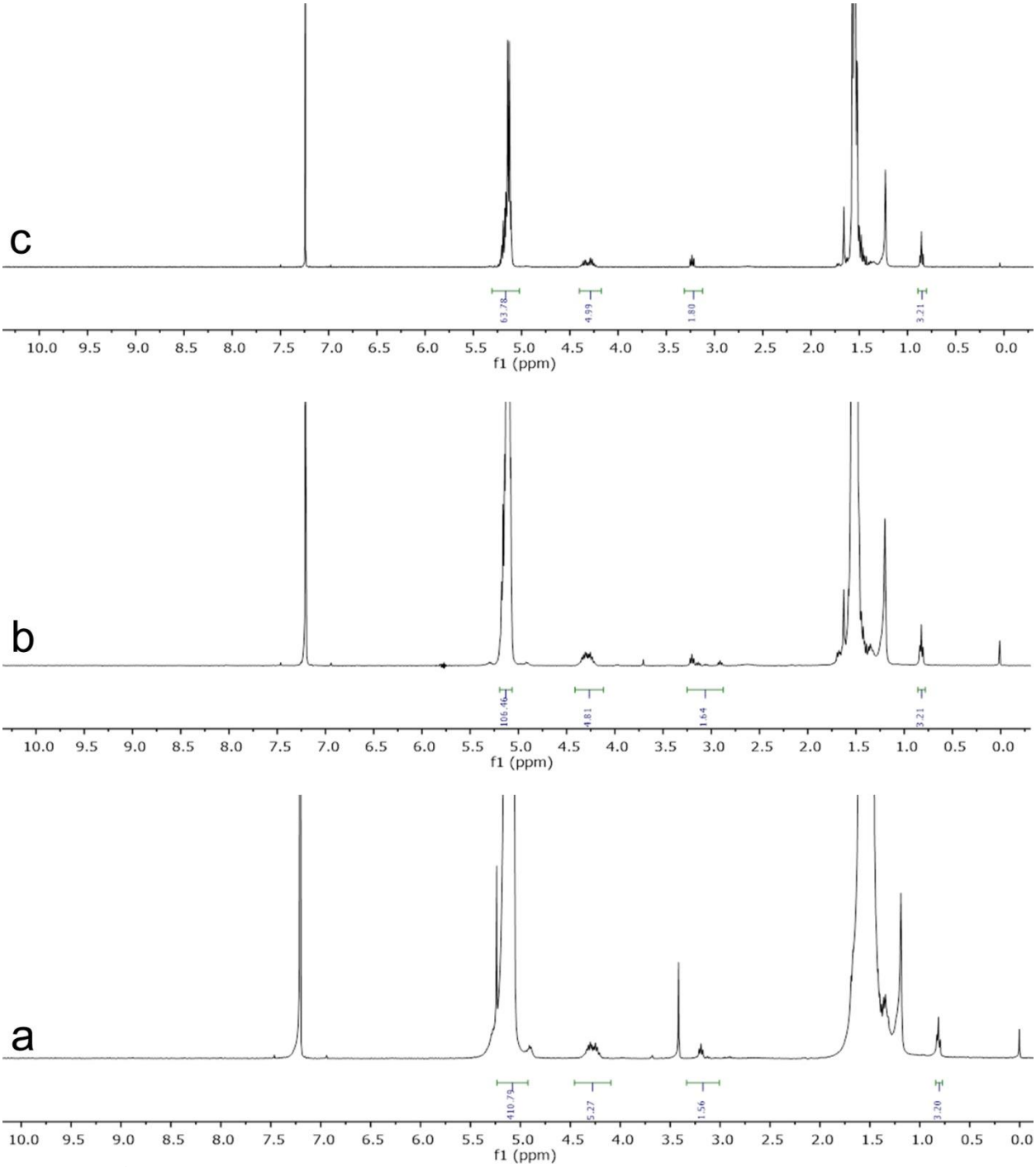

Figure S6. ^{1}H NMR (400 MHz, CDCl3) spectrum of (a) PLA-CTA-30, (b) PLA-CTA-8 and (c) PLA-CTA-5.

Table S4. Composition of the polymerization mixtures, yield and weight loss of the cross-linked precursors by basic etching

Entry	CPPs	Polymerization mixture				Precursor yield (%)	Weight loss (%)
		PLA-CTA (g)	Styrene (g)	MVCL (g)	DMF (mL)		
1	CPP(30/DVB)	0.16	0.29	0.09	0.1	63[a]	39
2	CPP(30/2VBP)	0.19	0.30	0.15	0.3	97	38
3	CPP(30/3VPB)	0.16	0.20	0.18	0.6	98	39
4	CPP(30/4VBM)	0.18	0.15	0.26	0.8	98	36
5	CPP(8/DVB)	0.16	0.29	0.09	0.1	79 [a]	43
6	CPP(8/2VBP)	0.19	0.30	0.15	0.3	98	34
7	CPP(8/3VPB)	0.16	0.20	0.18	0.6	99	35
8	CPP(8/4VBM)	0.18	0.15	0.26	0.8	99	36
9	CPP(5/DVB)	0.16	0.29	0.09	0.1	66[a]	41
10	CPP(5/2VBP)	0.19	0.30	0.15	0.3	99	37
11	CPP(5/3VPB)	0.16	0.20	0.18	0.6	99	35
12	CPP(5/4VBM)	0.18	0.15	0.26	0.8	98	38

[a]Insoluble white materials were formed on top of the polymerization mixture and attributed formation of P(S-co-DVB) not mediated by the RAFT CTA.

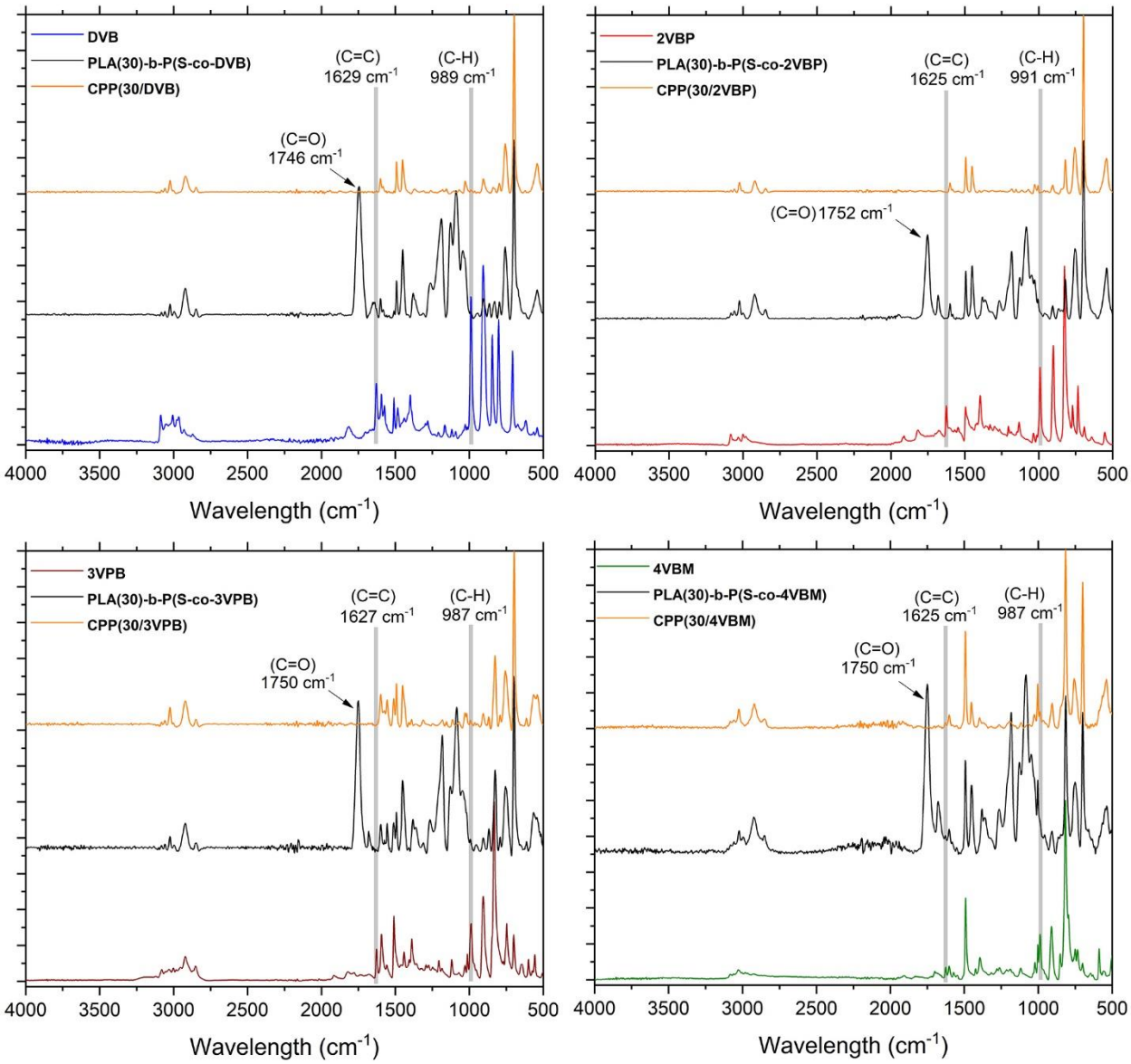

Figure S7. FTIR spectra of DVB (blue), 2VBP (red), 3VPB (brown), 4VBM (green), PLA(30)-b-(S-co-MVCL) (black) and corresponding CPP(30/MVCL) (orange).

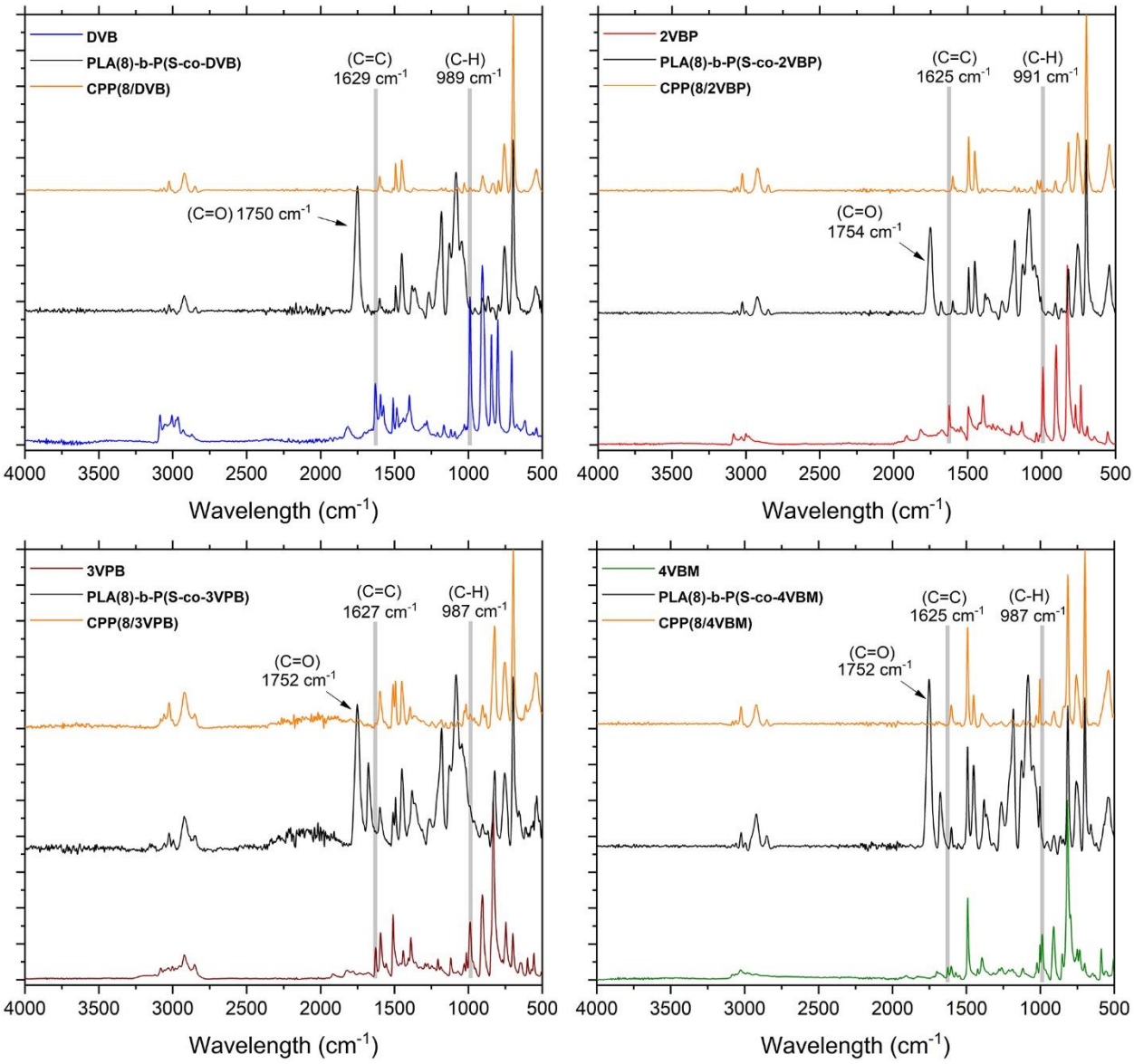

Figure S8. FTIR spectra of DVB (blue), 2VBP (red), 3VPB (brown), 4VBM (green), PLA(8)-b-(S-co-MVCL) (black) and corresponding CPP(8/MVCL) (orange).

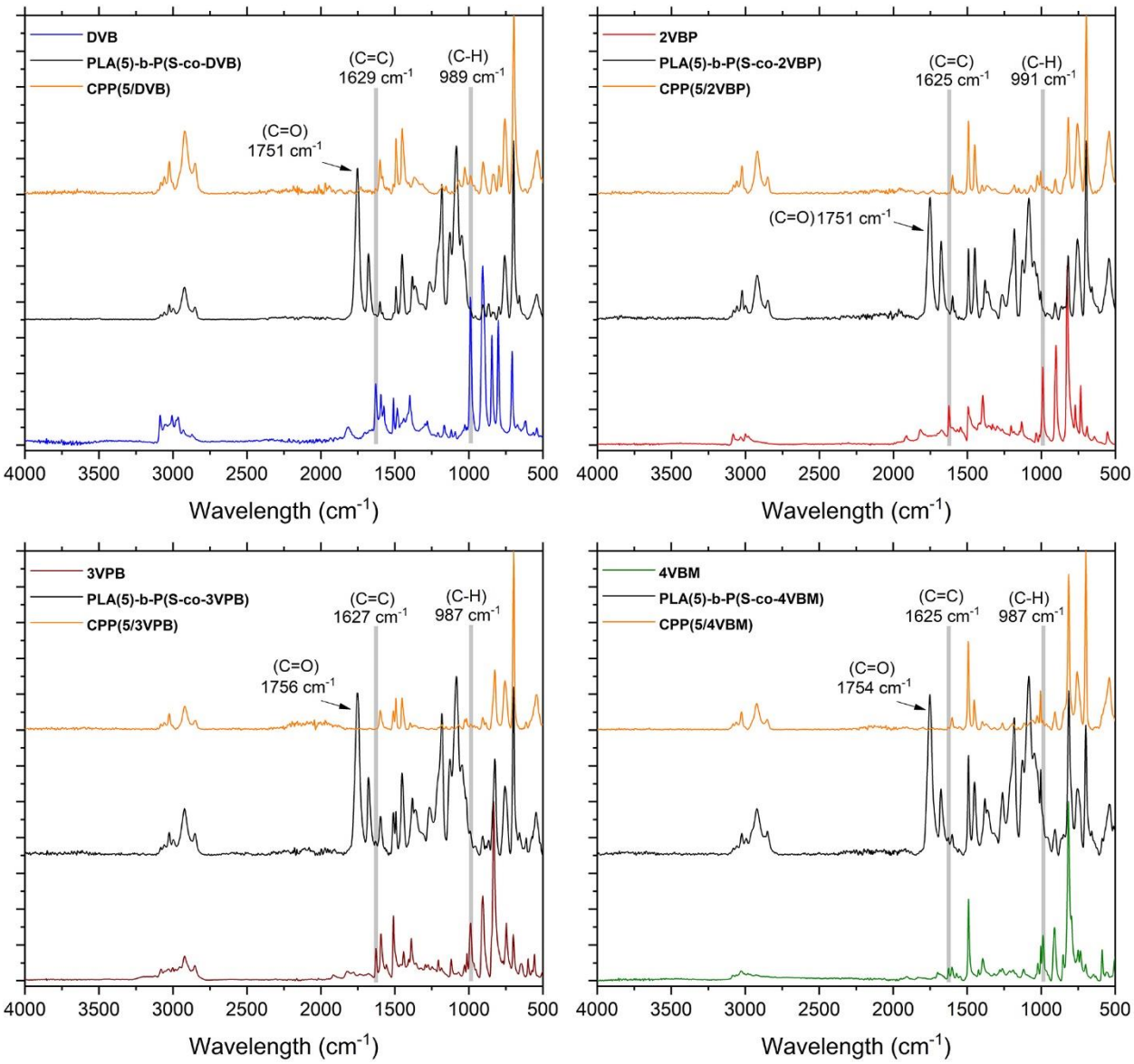

Figure S9. FTIR spectra of DVB (blue), 2VBP (red), 3VPB (brown), 4VBM (green), PLA(5)-b-(S-co-MVCL) (black) and corresponding CPP(5/MVCL) (orange).

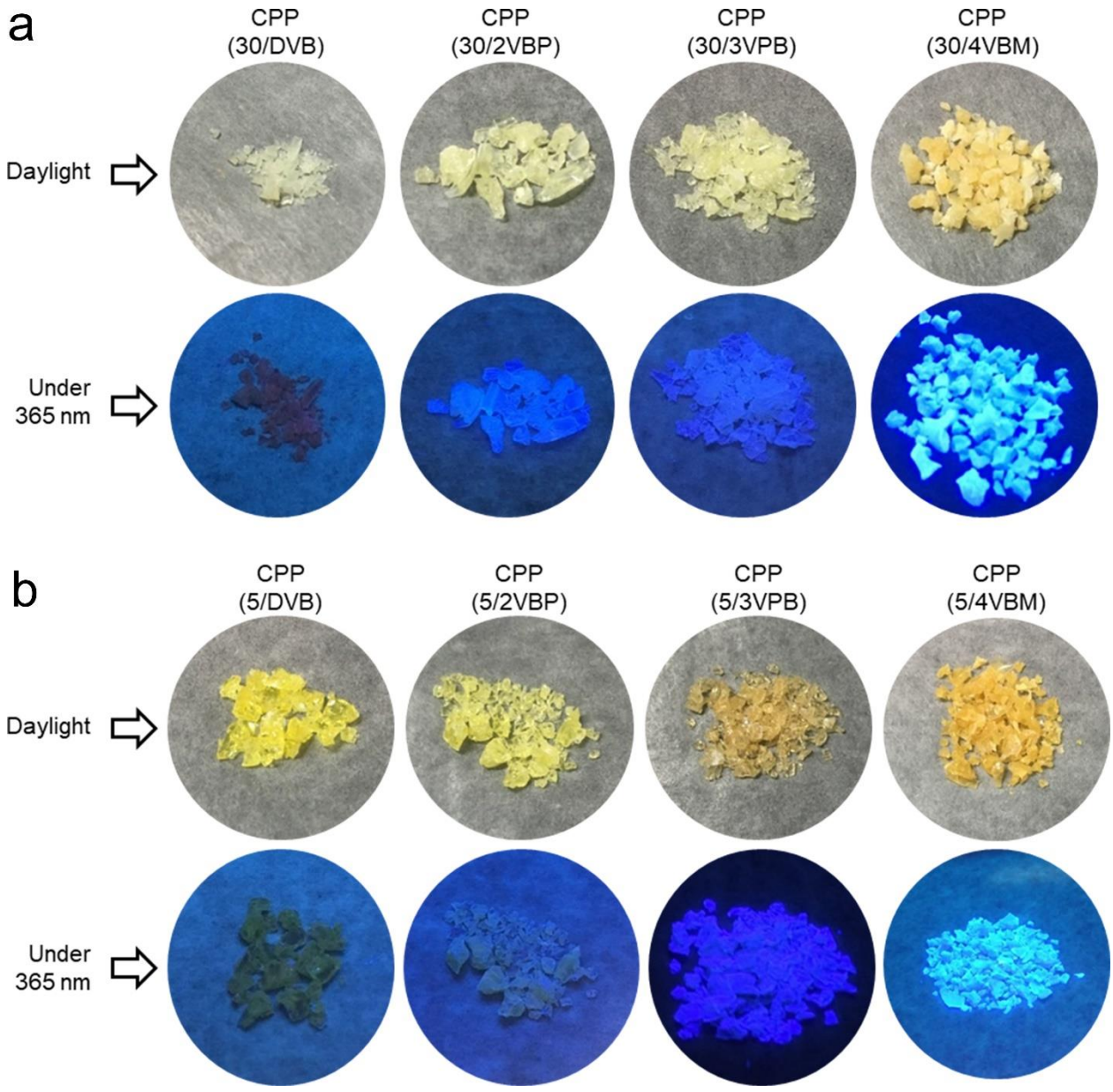

Figure S10. Photo of (a) CPP(30/MVCL)s and (b) CPP(5/MVCL)s under daylight and UV (365 nm).

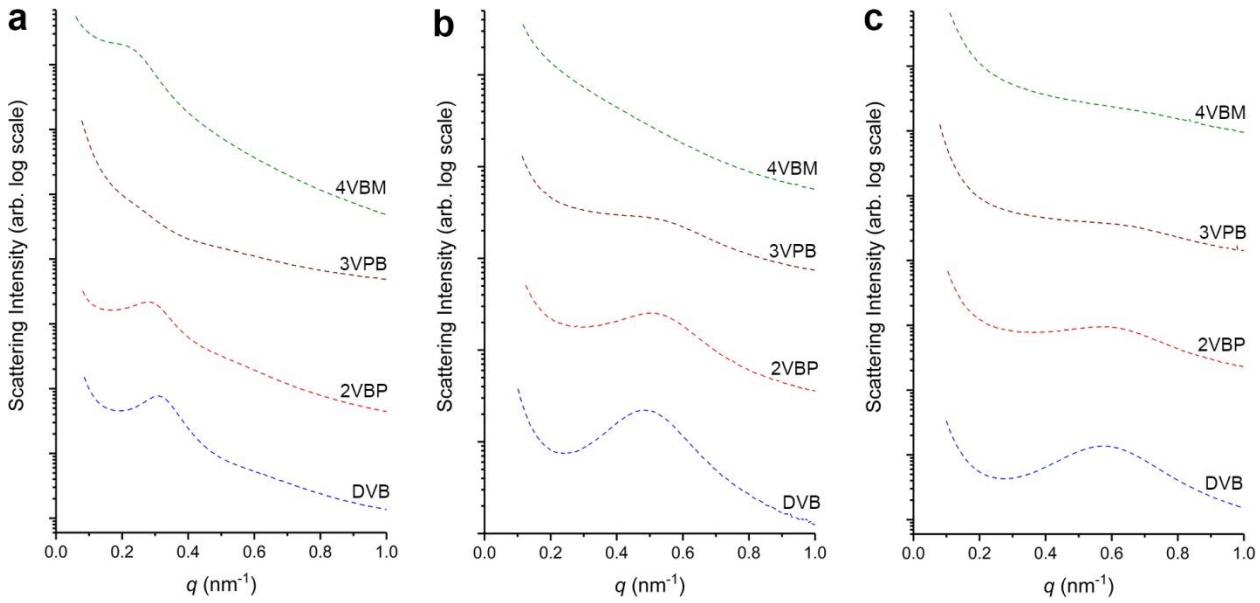

Figure S11. SAXS data of PLA-b-(S-co-MVCL)s synthesized with different PLA-CTAs. (a) PLA-CTA-30. (b) PLA-CTA-8. (c) PLA-CTA-5.

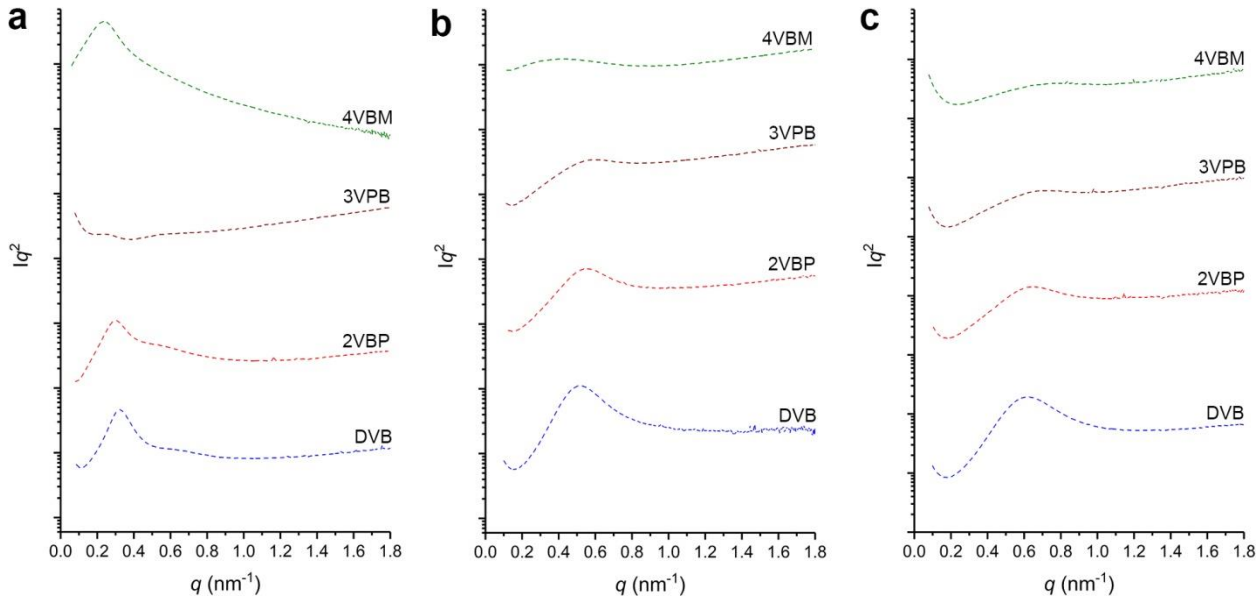

Figure S12. Lorentz-corrected SAXS data of PLA-b-(S-co-MVCL)s synthesized with different PLA-CTAs. (a) PLA-CTA-30. (b) PLA-CTA-8. (c) PLA-CTA-5.

Table S5. Position of the SAXS principal peak (q^*) and domain spacing (d) of PLA-b-P(S-co-MVCL)

Precursor	q^* (nm^{-1})	d (nm)
PLA(30)-b-(S-co-DVB)	0.31	20
PLA(30)-b-(S-co-2VBP)	0.28	21
PLA(30)-b-(S-co-3VPB)	0.26	24
PLA(30)-b-(S-co-4VBM)	0.21	30
PLA(8)-b-(S-co-DVB)	0.49	13
PLA(8)-b-(S-co-2VBP)	0.51	12
PLA(8)-b-(S-co-3VPB)	0.53	12
PLA(8)-b-(S-co-4VBM)	0.44	14
PLA(5)-b-(S-co-DVB)	0.58	11
PLA(5)-b-(S-co-2VBP)	0.62	10
PLA(5)-b-(S-co-3VPB)	0.66	9
PLA(5)-b-(S-co-4VBM)	0.67	9

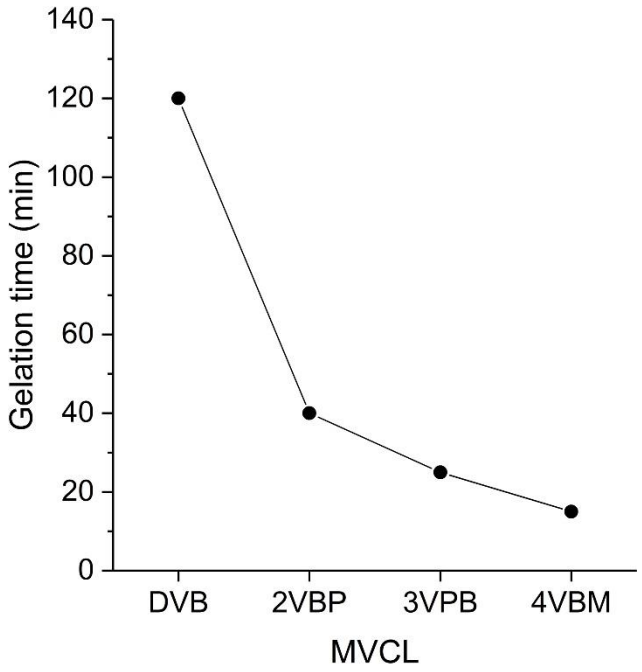

Figure S13. Gelation time of the polymerization mixtures containing different MVCLs.

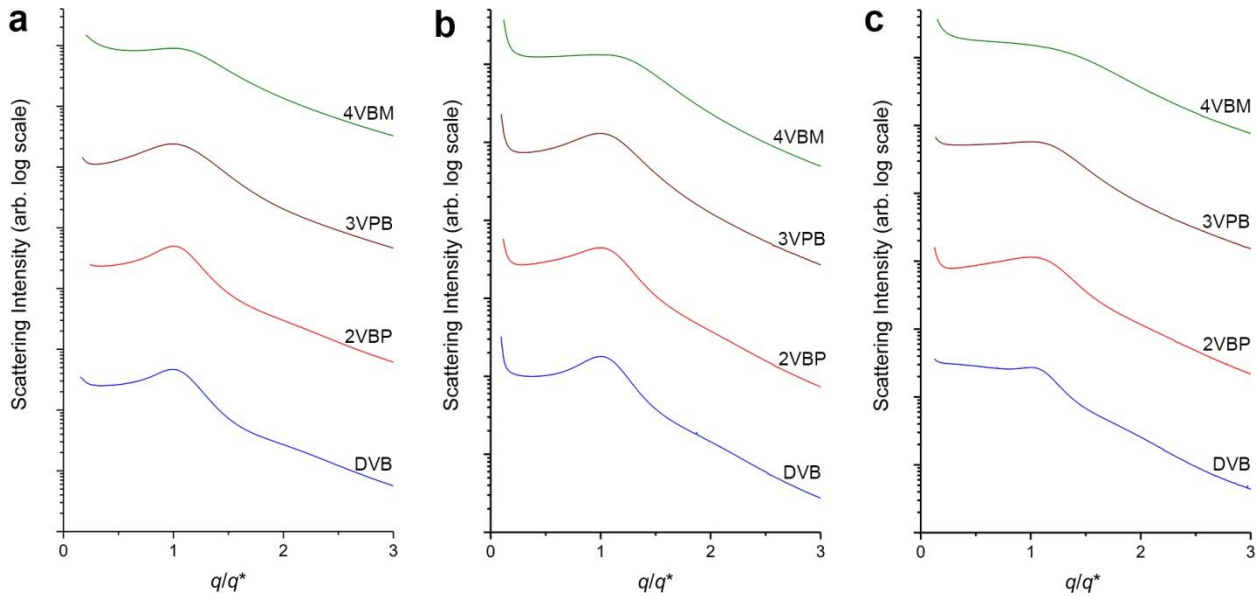

Figure S14. Scaled SAXS data of (a) CPP(30/MVCL) (b) CPP(8/MVCL) and (c) CPP(5/MVCL). The SAXS data have been vertically shifted for clarity.

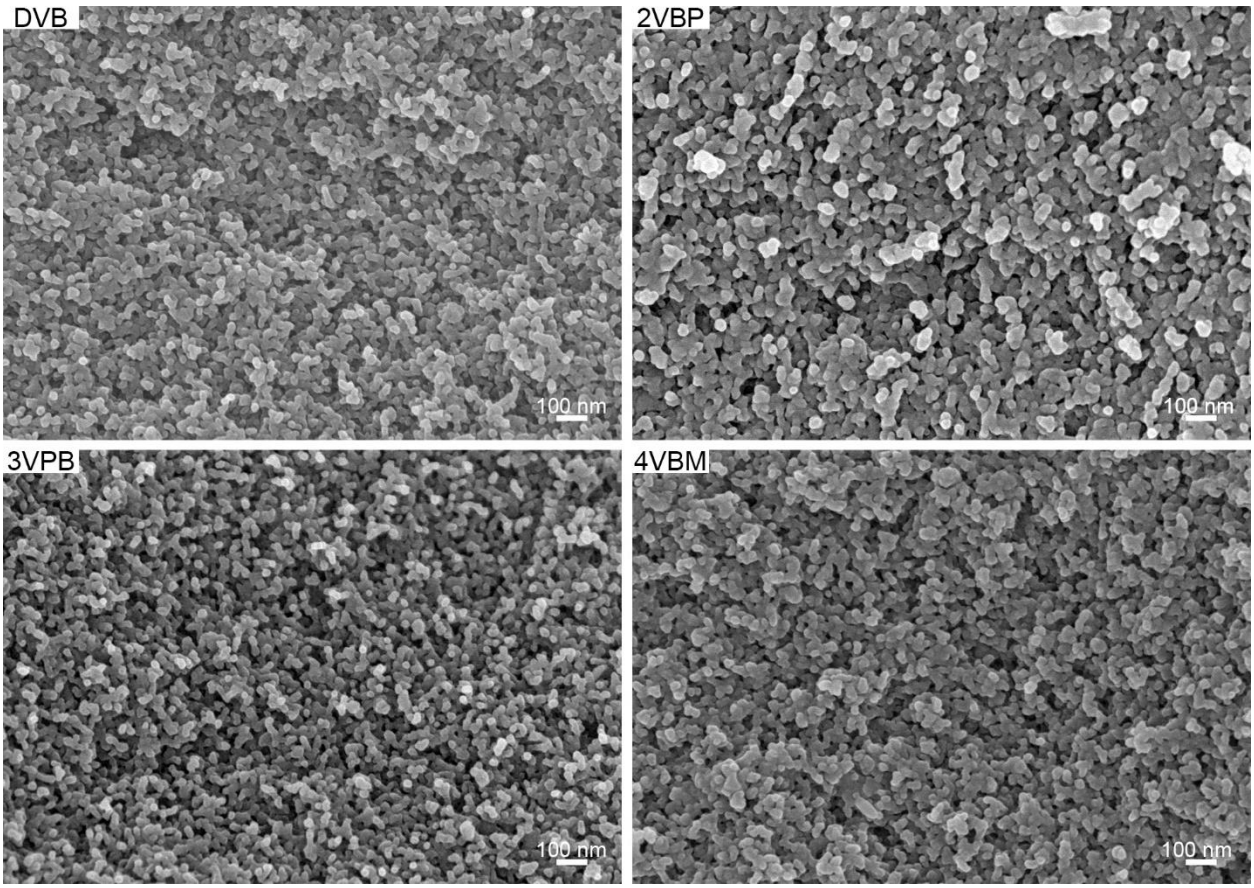

Figure S15. SEM images of CPP(30/MVCL)s.

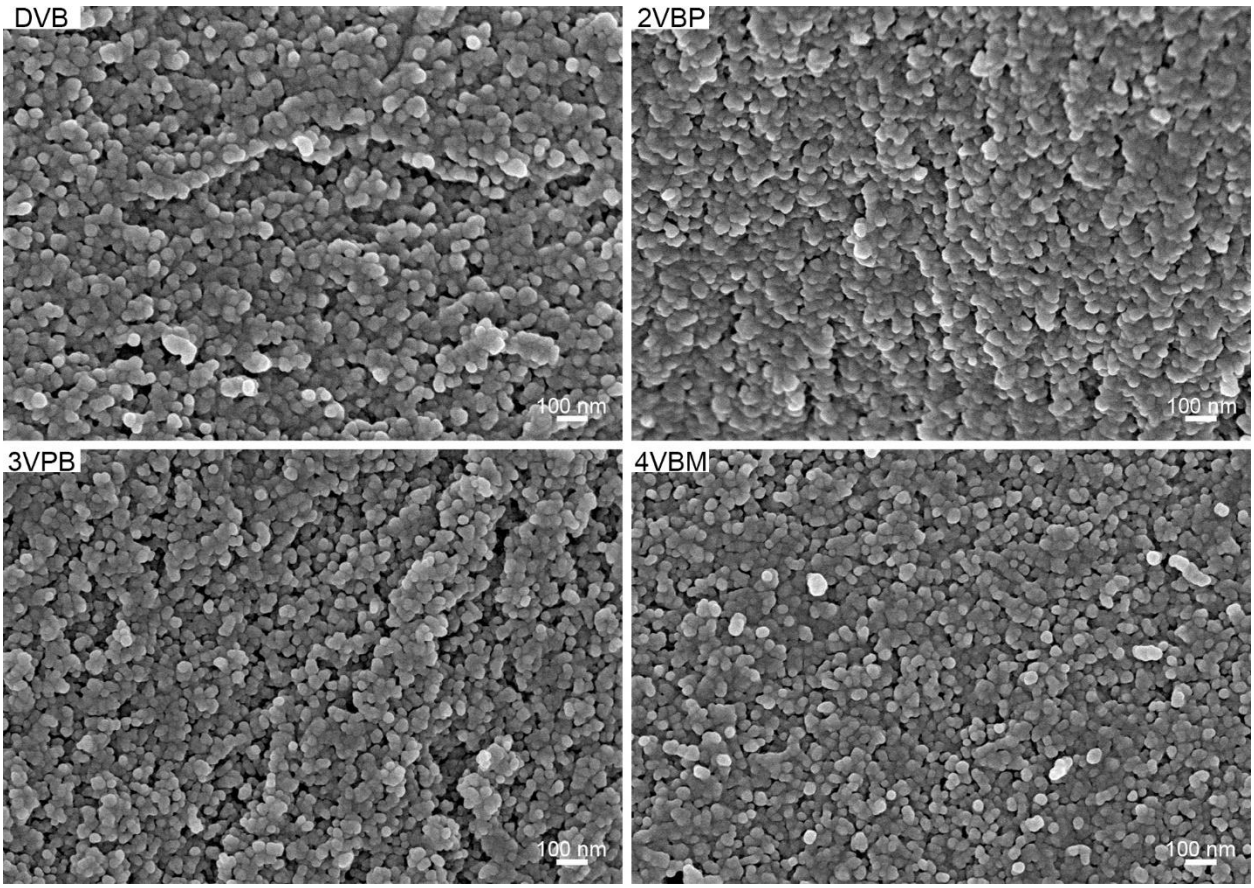

Figure S16. SEM images of CPP(5/MVCL)s.

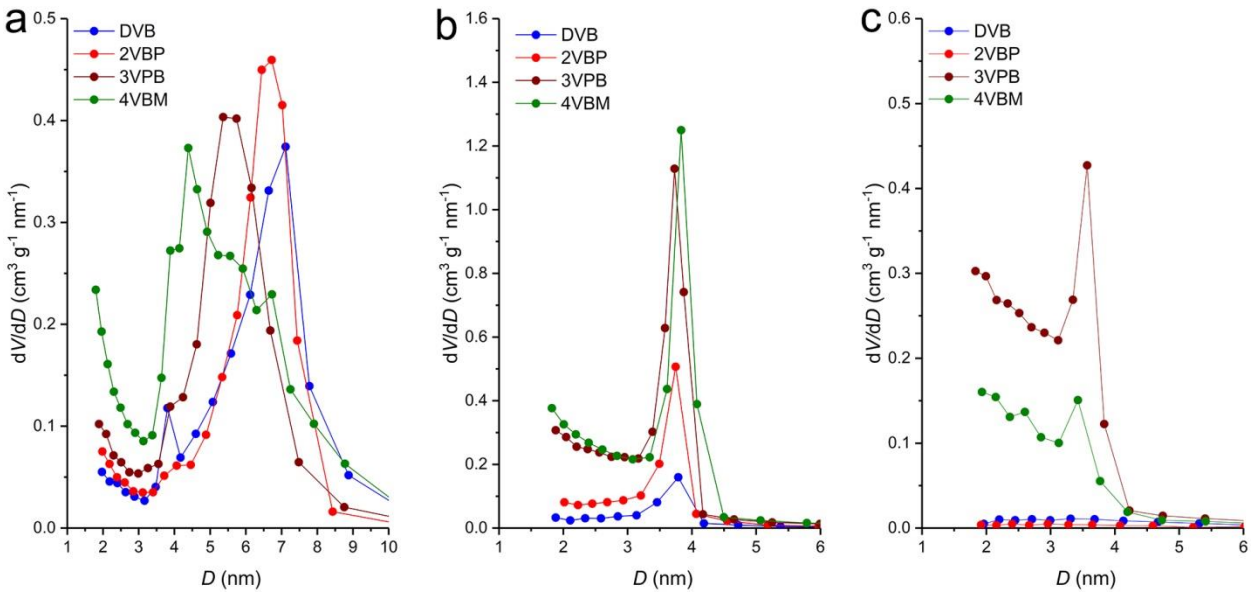

Figure S17. BJH pore size distributions of the desorption branch of the isotherms (a) CPP(30/MVCL)s, (b) CPP(8/MVCL)s and (c) CPP(5/MVCL)s.

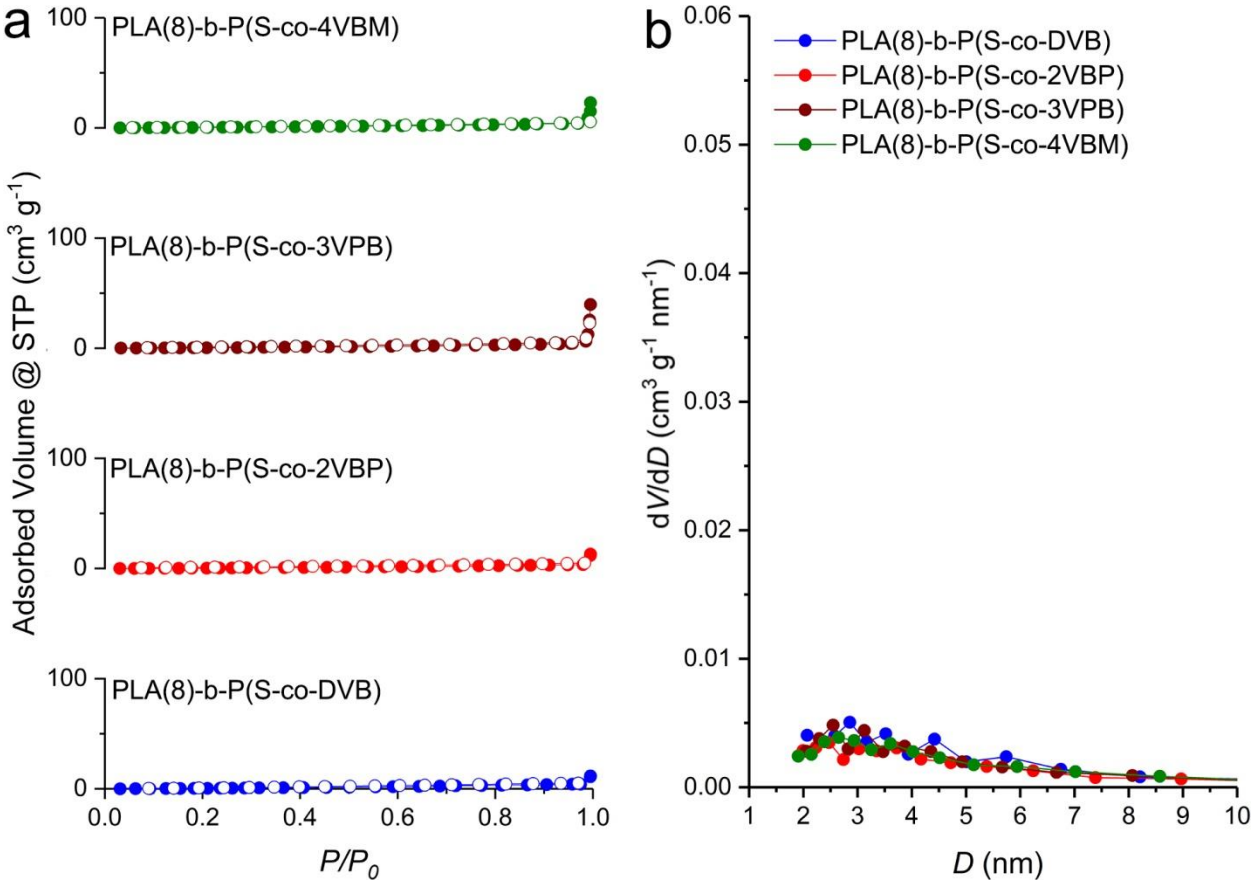

Figure S18. (a) Nitrogen adsorption isotherms of PLA(8)-b-P(S-co-MVCL)s. Filled circles: adsorption. Empty circles: desorption. (b) BJH pore size distributions of the desorption branch of the isotherms.

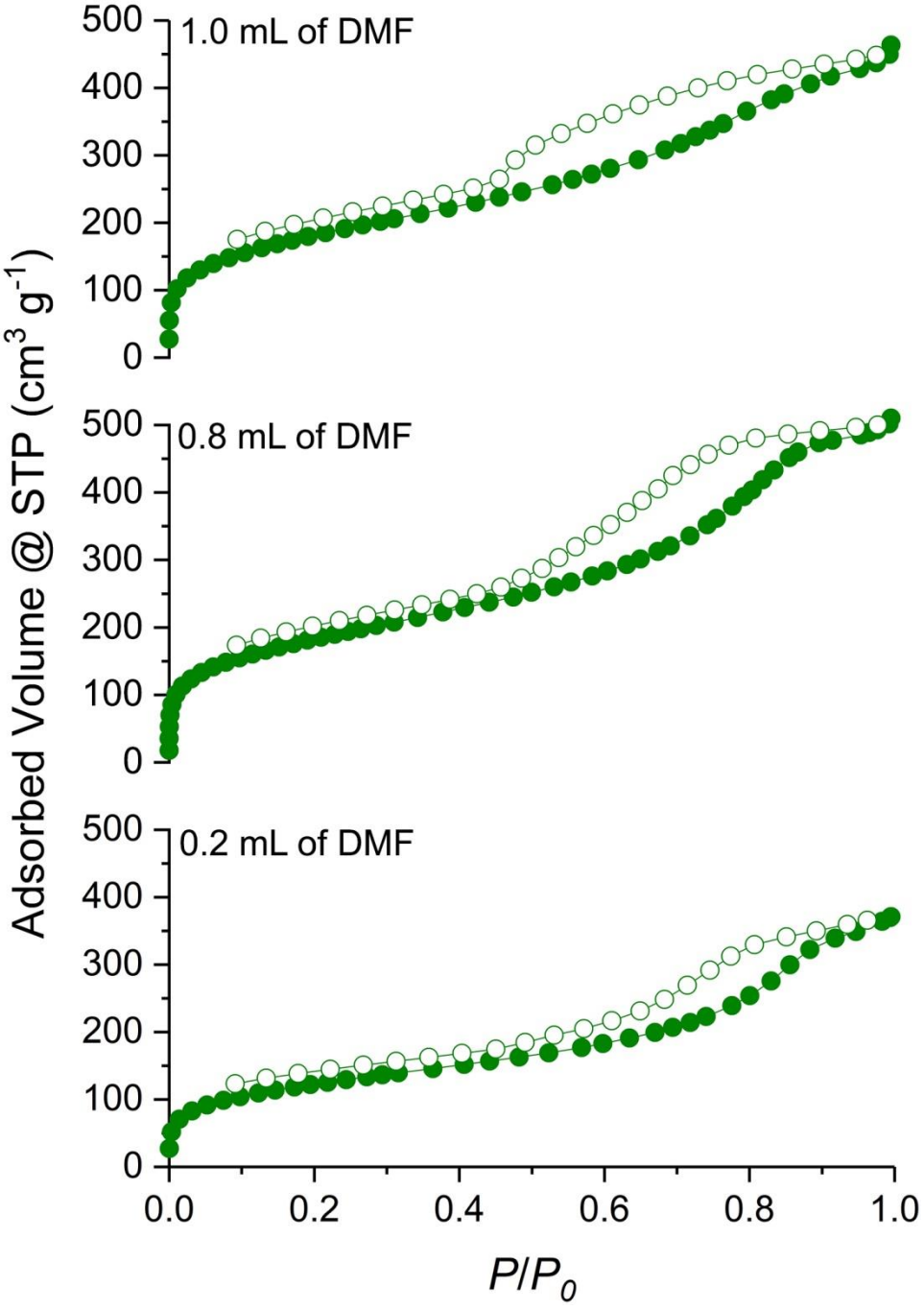

Figure S19. Nitrogen adsorption isotherms of CPP(30/4VBM) synthesized with 0.2 mL, 0.8 mL (same data shown in Figure 4a), and 1.0 mL of DMF. Filled circles: adsorption. Empty circles: desorption. S_{BET} values were 426, 632, and 624 $m^2\ g^{-1}$, respectively.

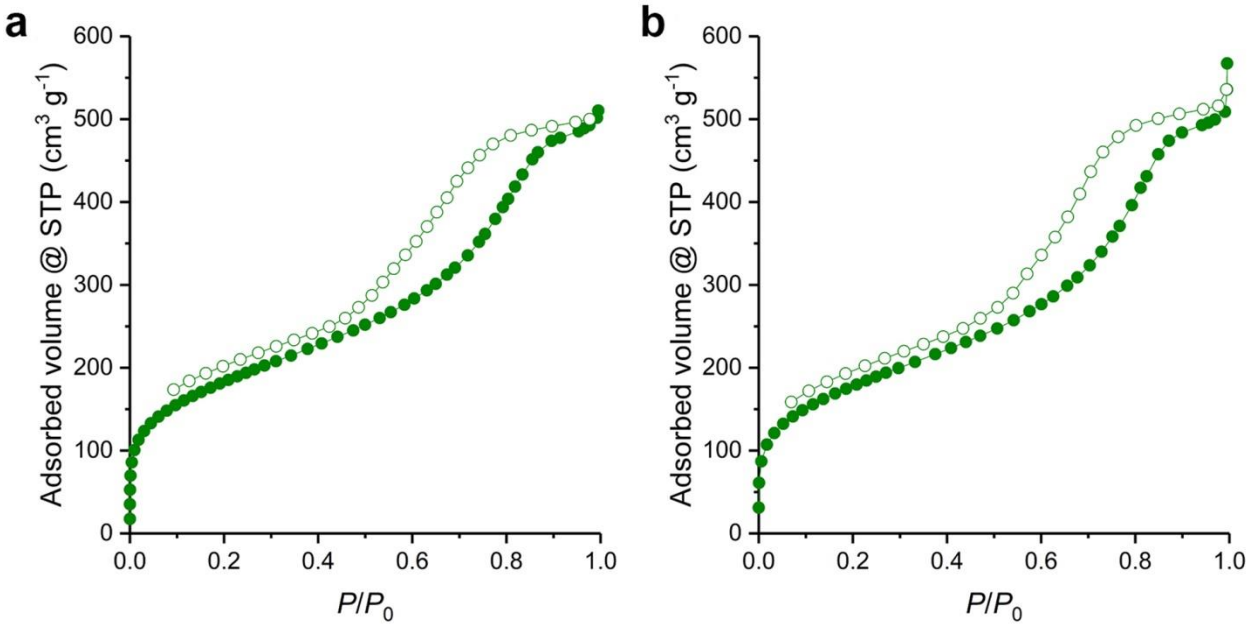

Figure S20. Nitrogen adsorption isotherms of CPP(30/4VBM) before (a) and after (b) heating at 100 °C for 1 h in air. Filled circles: adsorption. Empty circles: desorption. From each isotherm, S_{BET} and pore volume were estimated as 632 m^2 g^{-1} and 0.65 mL g^{-1} (a) and 620 m^2 g^{-1} 0.68 mL g^{-1} (b), respectively.